Photoinduced processes in dye-sensitized photoanodes under the spotlight: a multiscale in silico investigation

Menzel, J.P.

CHAPTER 2

Theoretical Background and Computational Methods

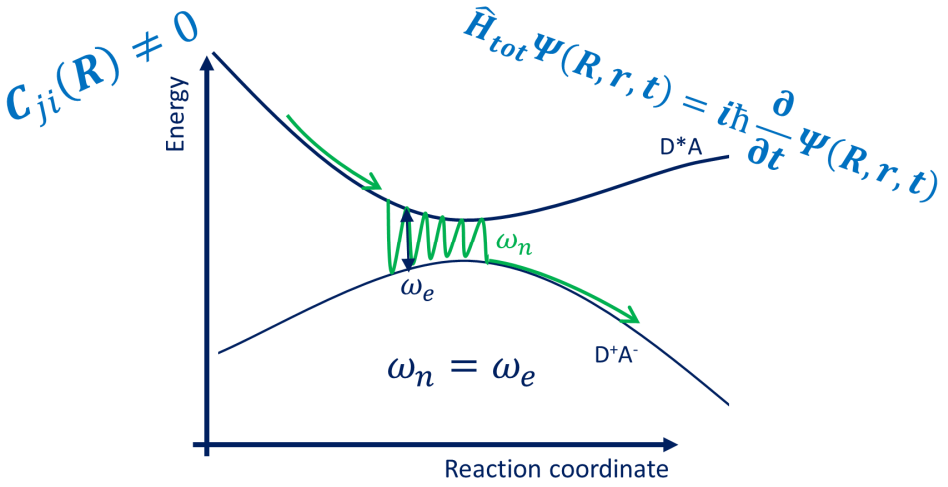

2

Simulating photoinduced processes involves transitions between electronic states. These non-adiabatic transitions go beyond the commonly used Born-Oppenheimer approximation of decoupled electronic and nuclear motions. To describe these processes, nonadiabatic effects need to be included. Due to the large diversity of system sizes and time scales within a Dye-Sensitized Photoanode, various computational methods are needed to bridge between these time and space ranges. In this chapter, the theoretical background and various computational methods used in the following chapters are introduced. If not noted otherwise, equations are given using atomic units.

2.1 The Born-Oppenheimer Approximation and Beyond

Any chemical system where relativistic effects are negligible can in principle be described by the time dependent Schrödinger equation:

$$\hat{H}_{\text{tot}}\Psi(\boldsymbol{R},\boldsymbol{r},t) = i\frac{\partial}{\partial t}\Psi(\boldsymbol{R},\boldsymbol{r},t) \tag{2.01}$$

where i is the imaginary unit, Ψ the total wavefunction describing all nuclei with coordinates $\boldsymbol{R}$ and electrons with coordinates $\boldsymbol{r}$. The total Hamiltonian $\hat{H}_{\text{tot}}$ contains the kinetic energy operators for all n electrons and N nuclei as well as electrostatic interactions between them:

$$\hat{H}_{\text{tot}} = \hat{T}_{\text{el}} + \hat{T}_{\text{nuc}} + \hat{V}_{\text{el,el}} + \hat{V}_{\text{nuc,nuc}} + \hat{V}_{\text{el,nuc}}$$

$$= -\sum_{i=1}^{n}\frac{\nabla_{\boldsymbol{r}_n}^2}{2} - \sum_{I=1}^{N}\frac{\nabla_{\boldsymbol{R}_N}^2}{2M_I} + \sum_{i=1}^{n}\sum_{j>i}^{n}\frac{1}{|\boldsymbol{r_i} - \boldsymbol{r_j}|}$$

$$+ \sum_{I=1}^{N}\sum_{J>I}^{N}\frac{Z_I Z_J}{|\boldsymbol{R}_I - \boldsymbol{R}_J|} - \sum_{i=1}^{n}\sum_{I=1}^{N}\frac{Z_I}{|\boldsymbol{R}_I - \boldsymbol{r}_i|} \tag{2.02}$$

Here, capital indices denote nuclei while small indices denote electrons. Consequently, $\boldsymbol{R}_I$ describes the coordinates of nucleus I, Z_I its nuclear charge and M_I the mass ratio of its nuclear mass m_I to the electron mass m_e ($M_I = \frac{m_I}{m_e}$). Similarly, $\boldsymbol{r}_i$ are the coordinates of electron i, with its charge and mass already defined within the atomic units. Solving the time-dependent Schrödinger equation in practice cannot be done without further simplifications. One of the most crucial approximations of the last century that made it possible to investigate and evaluate a myriad of chemical systems is the Born-Oppenheimer approximation (BOA).[1]

Within the BOA the separation between energy levels is considered large compared to the kinetic energy of the nuclei. Due to the large mass mismatch between electrons and nuclei, the electrons readjust instantaneously to new nuclear coordinates, decoupling electronic and nuclear subsystems. In the BOA the total

wavefunction $\Psi(\boldsymbol{R},\boldsymbol{r},t)$ can be separated into a set of pseudo time-independent electronic states $\psi_i(\boldsymbol{r};\boldsymbol{R})$ and time-dependent nuclear wave functions $\chi_i(\boldsymbol{R},t)$:

$$\Psi(\boldsymbol{R},\boldsymbol{r},t) = \sum_{i=1}^{\infty} \psi_i(\boldsymbol{r};\boldsymbol{R})\chi_i(\boldsymbol{R},t)\,, \tag{2.03}$$

where the semicolon denotes a parametrical dependence of the electronic wavefunction on the nuclear coordinates and the index i runs over the entire set of electronic eigenfunctions. The BOA provides a separation of time and spatial coordinates for the electronic motion by splitting the electron-nuclear quantum space into two subsystems: a time dependent nuclear subsystem and a time-independent electronic subsystem that readjusts instantaneously to new nuclear coordinates. For the electronic subsystem the time-independent Schrödinger equation is used:

$$\hat{H}_{\mathrm{el}}\psi_i(\boldsymbol{r};\boldsymbol{R}) = \varepsilon_i\psi_i(\boldsymbol{r};\boldsymbol{R}) \tag{2.04}$$

with

$$\hat{H}_{\mathrm{el}} = \hat{T}_{\mathrm{el}} + \hat{V}_{\mathrm{el,el}} + \hat{V}_{\mathrm{nuc,nuc}} + \hat{V}_{\mathrm{el,nuc}} \tag{2.05}$$

The nuclear subsystem keeps its direct time dependence. Inserting equations 2.03 and 2.05 into the Schrödinger equation (equation 2.01) gives

$$\left(\hat{H}_{\mathrm{el}}+\hat{T}_{\mathrm{nuc}}\right)\sum_{i=1}^{\infty}\psi_i(\boldsymbol{r};\boldsymbol{R})\chi_i(\boldsymbol{R},t) = i\frac{\partial}{\partial t}\sum_{i=1}^{\infty}\psi_i(\boldsymbol{r};\boldsymbol{R})\chi_i(\boldsymbol{R},t) \tag{2.06}$$

Multiplying with the complex conjugate ψ_j^* and integrating with $\boldsymbol{r}$ over the entire space Ω_{tot} gives

$$\int_{\Omega_{\mathrm{tot}}} d\boldsymbol{r}\,\psi_j^*(\boldsymbol{r};\boldsymbol{R})\left(\hat{H}_{\mathrm{el}}+\hat{T}_{\mathrm{nuc}}\right)\sum_{i=1}^{\infty}\psi_i(\boldsymbol{r};\boldsymbol{R})\chi_i(\boldsymbol{R},t)$$

$$= \int_{\Omega_{\mathrm{tot}}} d\boldsymbol{r}\psi_j^*(\boldsymbol{r};\boldsymbol{R})\,i\frac{\partial}{\partial t}\sum_{i=1}^{\infty}\psi_i(\boldsymbol{r};\boldsymbol{R})\chi_i(\boldsymbol{R},t) \tag{2.07}$$

The term on the right side, as χ_i is independent of $\boldsymbol{r}$, becomes

$$i\frac{\partial}{\partial t}\sum_{i=1}^{\infty}\chi_i(\boldsymbol{R},t)\int_{\Omega_{\text{tot}}} d\boldsymbol{r}\,\psi_j^*(\boldsymbol{r};\boldsymbol{R})\psi_i(\boldsymbol{r};\boldsymbol{R}) = i\frac{\partial}{\partial t}\sum_{i=1}^{\infty}\chi_i(\boldsymbol{R},t)\delta_{ij}$$
$$= i\frac{\partial}{\partial t}\chi_j(\boldsymbol{R},t) \tag{2.08}$$

For the left side of eq. 2.7, two terms, one with $\widehat{H}_{\text{el}}$ and $\widehat{T}_{\text{nuc}}$ remain with the first one being

$$\int_{\Omega_{\text{tot}}} d\boldsymbol{r}\,\psi_j^*(\boldsymbol{r},\boldsymbol{R})\widehat{H}_{\text{el}}\sum_{i=1}^{\infty}\psi_i(\boldsymbol{r};\boldsymbol{R})\chi_i(\boldsymbol{R},t)$$
$$= \int_{\Omega_{\text{tot}}} d\boldsymbol{r}\,\psi_j^*(\boldsymbol{r};\boldsymbol{R})\sum_{i=1}^{\infty}\varepsilon_i(\boldsymbol{R})\psi_i(\boldsymbol{r};\boldsymbol{R})\chi_i(\boldsymbol{R},t)$$
$$= \sum_{i=1}^{\infty}\varepsilon_i(\boldsymbol{R})\chi_i(\boldsymbol{R},t)\delta_{ji} = \varepsilon_j(\boldsymbol{R})\chi_j(\boldsymbol{R},t) \tag{2.09}$$

The second term can be simplified through the chain rule:

$$\int_{\Omega_{\text{tot}}} d\boldsymbol{r}\,\psi_j^*(\boldsymbol{r};\boldsymbol{R})\widehat{T}_{\text{nuc}}\sum_{i=1}^{\infty}\psi_i(\boldsymbol{r};\boldsymbol{R})\chi_i(\boldsymbol{R},t)$$
$$= \int_{\Omega_{\text{tot}}} d\boldsymbol{r}\,\psi_j^*(\boldsymbol{r};\boldsymbol{R})\left(-\sum_{I=1}^{N}\frac{\nabla_{\boldsymbol{R}}^2}{2M_I}\right)\sum_{i=1}^{\infty}\psi_i(\boldsymbol{r};\boldsymbol{R})\chi_i(\boldsymbol{R},t)$$
$$= \int_{\Omega_{\text{tot}}} d\boldsymbol{r}\,\psi_j^*(\boldsymbol{r};\boldsymbol{R})\left(-\sum_{I=1}^{N}\frac{1}{2M_I}\right)\sum_{i=1}^{\infty}(\nabla_{\boldsymbol{R}}^2\psi_i(\boldsymbol{r};\boldsymbol{R}))\chi_i(\boldsymbol{R},t)$$
$$+ 2\int_{\Omega_{\text{tot}}} d\boldsymbol{r}\,\psi_j^*(\boldsymbol{r};\boldsymbol{R})\left(-\sum_{I=1}^{N}\frac{1}{2M_I}\right)\sum_{i=1}^{\infty}\big(\nabla_{\boldsymbol{R}}\psi_i(\boldsymbol{r};\boldsymbol{R})\big)\big(\nabla_{\boldsymbol{R}}\chi_i(\boldsymbol{R},t)\big)$$
$$+ \int_{\Omega_{\text{tot}}} d\boldsymbol{r}\,\psi_j^*(\boldsymbol{r};\boldsymbol{R})\left(-\sum_{I=1}^{N}\frac{1}{2M_I}\right)\sum_{i=1}^{\infty}\psi_i(\boldsymbol{r};\boldsymbol{R})(\nabla_{\boldsymbol{R}}^2\chi_i(\boldsymbol{R},t))$$

$$= -\sum_{I=1}^{N} \frac{1}{2M_I} D_{ji}(\boldsymbol{R}) \sum_{i=1}^{\infty} \chi_i(\boldsymbol{R},t) - \sum_{I=1}^{N} \frac{1}{M_I} \boldsymbol{d}_{ji}(\boldsymbol{R}) \nabla_{\boldsymbol{R}} \sum_{i=1}^{\infty} \chi_i(\boldsymbol{R},t)$$

$$+ \sum_{i=1}^{\infty} \hat{T}_{\mathrm{nuc}} \chi_i(\boldsymbol{R},t) \delta_{ji}$$

$$= \sum_{i=1}^{\infty} \boldsymbol{C}_{ji}(\boldsymbol{R}) \chi_i(\boldsymbol{R},t) + \hat{T}_{\mathrm{nuc}} \chi_j(\boldsymbol{R},t) \tag{2.10}$$

with $\boldsymbol{C}_{ji}$ being the non-adiabatic coupling terms[2]

$$\boldsymbol{C}_{ji}(\boldsymbol{R}) = -\sum_{I=1}^{N} \frac{1}{2M_I} D_{ji}(\boldsymbol{R}) - \sum_{I=1}^{N} \frac{1}{M_I} \boldsymbol{d}_{ji}(\boldsymbol{R}) \nabla_{\boldsymbol{R}} \tag{2.11}$$

with respectively

$$D_{ji}(\boldsymbol{R}) = \int_{\Omega_{\mathrm{tot}}} d\boldsymbol{r}\, \psi_j^*(\boldsymbol{r};\boldsymbol{R}) \nabla_{\boldsymbol{R}}^2 \psi_i(\boldsymbol{r};\boldsymbol{R}) \tag{2.12}$$

being called the second order nonadiabatic coupling or kinetic coupling term and

$$\boldsymbol{d}_{ji}(\boldsymbol{R}) = \int_{\Omega_{\mathrm{tot}}} d\boldsymbol{r}\, \psi_j^*(\boldsymbol{r};\boldsymbol{R}) \nabla_{\boldsymbol{R}} \psi_i(\boldsymbol{r};\boldsymbol{R}) \tag{2.13}$$

the first order nonadiabatic coupling or derivative coupling term, which is a vector. It is important to note that both interactions couple between different electronic states ψ_i and ψ_j. Due to the high mass ratio in the prefactor in equation 2.11, the $\boldsymbol{C}_{ij}$ is assumed to be negligible in the BOA. As the nuclei are much heavier than the electrons, these are following the time-dependent potential energy landscape established by the nuclei, while remaining essentially in an electronic eigenstate that gradually develops over time. When inserting the results from equations 2.08, 2.09 and 2.10 into equation 2.07, we obtain

$$\left(\varepsilon_j(\boldsymbol{R}) + \hat{T}_{\mathrm{nuc}}\right) \chi_j(\boldsymbol{R},t) + \sum_{i=1}^{\infty} \boldsymbol{C}_{ji}(\boldsymbol{R}) \chi_i(\boldsymbol{R},t) = i \frac{\partial}{\partial t} \chi_j(\boldsymbol{R},t). \tag{2.14}$$

Finally, when assuming $C_{ji} = 0$, we end up with

$$\left(\varepsilon_j(\boldsymbol{R}) + \hat{T}_{\mathrm{nuc}}\right)\chi_j(\boldsymbol{R}, t) = i\frac{\partial}{\partial t}\chi_j(\boldsymbol{R}, t). \tag{2.15}$$

The nuclear wavefunctions are therefore propagated on adiabatic potential energy surfaces determined by the electronic system at nuclear positions $\boldsymbol{R}$. Neglecting $\boldsymbol{C}_{ji}$ allows for the approximate description of a wide variety of chemical problems where the chemistry proceeds while the system remains in the same electronic state. However, there are notable cases where this approximation breaks down and crossing involving different electronic states is essential to the chemical process.

Non-adiabaticity and Resonant Coupling between Nearly Degenerate Electronic States and Nuclear Vibrations

The BOA, allowing for efficient electronic structure methods and ab initio molecular dynamics (AIMD), has without a doubt led to deep insight into chemical problems and properties over time.[3–5] There are, however, significant limitations to its applicability. Employing the Hellman-Feynman theorem as described in reference [6] by Habitz and Votava, the first order terms of the non-adiabatic coupling $\boldsymbol{d}_{ji}$ can be expressed via the adiabatic states of the electronic system:

$$\boldsymbol{d}_{ji}(\boldsymbol{R}) = \frac{\int_{\Omega_{\mathrm{tot}}} d\boldsymbol{r}\, \psi_j^*(\boldsymbol{r}; \boldsymbol{R}) \nabla_{\boldsymbol{R}} \hat{H}_{\mathrm{el}} \psi_i(\boldsymbol{r}; \boldsymbol{R})}{\varepsilon_i - \varepsilon_j} \tag{2.16}$$

In this expression one can already see that the non-adiabatic coupling becomes non negligible for nearly degenerate adiabatic states. Here the BOA criterion that the energy difference is large compared to the kinetic energy of the nuclei is invalidated and the off-diagonal coupling between electronic and nuclear subsystem called nonadiabatic coupling becomes significant. A small energy difference between the electronic adiabatic states leads to an increase of the non-adiabatic terms in eq. 2.16.

If a nuclear mode with a frequency ω_{n} corresponding to the energy difference between these two states $\varepsilon_2 - \varepsilon_1 = \varepsilon_{\mathrm{e}} = \omega_{\mathrm{e}}$ is available in the system, this nuclear mode can couple to the electronic system and drive population transfer from one

state to another. This corresponds to Rabi oscillations[7] of the state populations induced by the nuclear vibration. Since this mode reaches resonance ($\omega_{\mathrm{n}} = \omega_{\mathrm{e}}$), it is filtered out by the system, effectively truncating the Hamiltonian , resulting in a system that can be represented by these two states only.[8] Inserting the nuclear wave functions $\chi_i(R,t)$ into equation 2.14 and employing a quantum-classical treatment where we exchange the quantum mechanical operators of the nuclear system by classical variables[9]

$$\begin{aligned} -\frac{\boldsymbol{d}_{ij}}{M}\nabla_R &\rightarrow -i\frac{\boldsymbol{d}_{ij}}{M}\boldsymbol{p} \\ -\frac{D_{ij}}{2M} &\rightarrow \frac{p^2}{2M}\delta_{ij} \\ \hat{T}_{\mathrm{nuc}} &\rightarrow \frac{p^2}{2M} \end{aligned} \tag{2.17}$$

the time-dependent Schrödinger equation of motion can be represented by a set of coupled equations[9]

$$\sum_{i=1}^{\infty}\left\{\varepsilon_i(\boldsymbol{R})\delta_{ji} - i\frac{\boldsymbol{p}}{M}\boldsymbol{d}_{ji}(\boldsymbol{R})\right\}\chi_i(\boldsymbol{R},t) = i\frac{\partial}{\partial t}\chi_j(\boldsymbol{R},t). \tag{2.18}$$

When a single, long living resonant mode is filtered out from a system with slowly varying geometry (i.e. the overall variation of the nuclear system measured by $\boldsymbol{R}$ is small on the timescale of the resonant nonadiabatic process) to couple two electronic states in a quasi-static environment, the displacement R_0 along the ω_{n} normal coordinate, phase φ and momentum $p = -MR_0\omega_{\mathrm{n}}\sin(\omega_{\mathrm{n}}t - \varphi)$ lead to[8]

$$\sum_{i=1,2}\left\{\varepsilon_i(R_0)\delta_{ji} + iR_0 d_{ji}(\boldsymbol{R})\omega_{\mathrm{n}}\sin(\omega_{\mathrm{n}}t - \varphi)\right\}\chi_i(\boldsymbol{R},t) = i\frac{\partial}{\partial t}\chi_j(\boldsymbol{R},t) \tag{2.19}$$

Where $d_{ji}(\boldsymbol{R})$ is now a scalar due to the multiplication with the momentum that corresponds to a single normal mode. Using equation 2.03, the two vibronic states can be represented by

$$\begin{aligned} \Psi_1(\boldsymbol{R},\boldsymbol{r},t) &= \chi_1(\boldsymbol{R},t)\psi_1(\boldsymbol{r};\boldsymbol{R}) \\ \Psi_2(\boldsymbol{R},\boldsymbol{r},t) &= \chi_2(\boldsymbol{R},t)\psi_2(\boldsymbol{r};\boldsymbol{R}) \end{aligned} \tag{2.20}$$

With only two states the equation of motion (2.19) reduces to the 2×2 matrix equation

$$\begin{pmatrix} \varepsilon_1 & iR_0 d_{12}(\boldsymbol{R})\omega_{\mathrm{n}} \sin(\omega_n t - \varphi) \\ iR_0 d_{21}(\boldsymbol{R})\omega_{\mathrm{n}} \sin(\omega_n t - \varphi) & \varepsilon_2 \end{pmatrix} \begin{pmatrix} \chi_1(\boldsymbol{R},t) \\ \chi_2(\boldsymbol{R},t) \end{pmatrix} = i\frac{\partial}{\partial t}\begin{pmatrix} \chi_1(\boldsymbol{R},t) \\ \chi_2(\boldsymbol{R},t) \end{pmatrix}. \tag{2.21}$$

It is convenient to position the energies of the electronic states symmetrically around zero so that $\varepsilon_1 = E, \varepsilon_2 = -E$, and choose a phase $\varphi = \frac{\pi}{2}$ at $t = 0$. With $d_{12} = -d_{21}$ and using the Pauli matrices

$$\begin{aligned} \hat{\sigma}_z &= \begin{pmatrix} 1 & 0 \\ 0 & -1 \end{pmatrix} = \hat{L}_z \\ \hat{\sigma}_z &= \begin{pmatrix} 1 & 0 \\ 0 & -1 \end{pmatrix} = \hat{L}_z \end{aligned} \tag{2.22}$$

which correspond to the angular momentum operators, we arrive at

$$\left(E\hat{L}_z - 2R_0 \boldsymbol{d}_{12}(\boldsymbol{R})\omega_{\mathrm{n}} \sin\left(\omega_{\mathrm{n}} t + \tfrac{\pi}{2}\right)\hat{L}_y\right)\begin{pmatrix} \chi_1(\boldsymbol{R},t) \\ \chi_2(\boldsymbol{R},t) \end{pmatrix} = i\frac{\partial}{\partial t}\begin{pmatrix} \chi_1(\boldsymbol{R},t) \\ \chi_2(\boldsymbol{R},t) \end{pmatrix}. \tag{2.23}$$

This matrix equation for the Hamiltonian is analogous to a system of a precessing fictitious spin S=1/2[8]

$$\widehat{H} = \left(\omega_e \hat{L}_z - 2R_0 d_{12}(\boldsymbol{R})\omega_{\mathrm{n}} \sin\left(\omega_{\mathrm{n}} t + \tfrac{\pi}{2}\right)\hat{L}_y\right) = \widehat{H}_0 + \widehat{H}_1. \tag{2.24}$$

The $\widehat{H}_0$ is the adiabatic term comprising the diagonal elements of the matrix, and the nonadiabatic $\widehat{H}_1$ comprises the off-diagonal terms that are time-dependent due to the nuclear motion with frequency ω_{n}. Non adiabatic transfer is enabled in cases where the electronic and nuclear frequencies approach, finally reaching resonance $\omega_{\mathrm{n}} = \omega_{\mathrm{e}}$, with the time scales of electronic and nuclear motion converging. This allows for removing the explicit time dependency of the equations of motion, by transforming the time dependent Hamiltonian to the interaction frame of the nuclear motion to make it time-independent. For this, the $2\sin\left(\omega_{\mathrm{n}} t + \frac{\pi}{2}\right)$ term can be dcomposed into two counter rotating components, which rotate along $\hat{L}_z$ in opposite directions:

$$2\sin\left(\omega_{\mathrm{n}}t+\frac{\pi}{2}\right)\hat{L}_y = 2\cos(\omega_{\mathrm{n}}t)\hat{L}_y = 2\cos(\omega_{\mathrm{n}}t)\hat{L}_y + \sin(\omega_{\mathrm{n}}t)\,\hat{L}_x - \sin(\omega_{\mathrm{n}}t)\,\hat{L}_x = \mathrm{e}^{-i\omega_{\mathrm{n}}t\hat{L}_z}\hat{L}_y\mathrm{e}^{i\omega_{\mathrm{n}}t\hat{L}_z} + \mathrm{e}^{i\omega_{\mathrm{n}}t\hat{L}_z}\hat{L}_y\mathrm{e}^{-i\omega_{\mathrm{n}}t\hat{L}_z}. \tag{2.25}$$

This leads to

$$\widehat{H}_1 = -R_0 d_{12}(\boldsymbol{R})\omega_{\mathrm{n}}\left(\mathrm{e}^{-i\omega_{\mathrm{n}}t\hat{L}_z}\hat{L}_y\mathrm{e}^{i\omega_{\mathrm{n}}t\hat{L}_z} + \mathrm{e}^{i\omega_{\mathrm{n}}t\hat{L}_z}\hat{L}_y\mathrm{e}^{-i\omega_{\mathrm{n}}t\hat{L}_z}\right). \tag{2.26}$$

The first term represents a transformation with a rotation around the z axis at frequency ω_{n}, while the second term rotates with a frequency of $-\omega_{\mathrm{n}}$. For the nuclear and electronic motion to couple, one of the two counter rotating components needs to reach resonance, while the other remains $2\omega_{\mathrm{n}}$ off resonance. In a physical, symmetric system, there is no inherent preference for one or the other component, suggesting that symmetry breaking is necessary for resonant coupling of a nuclear mode to drive population transfer between electronic states. This will be discussed further in chapter 3. Here, we assume the first term to couple to the electronic motion, while the second term is off resonance and can be neglected. To remove the time dependence of the Hamiltonian, we perform a unitary transformation with $\hat{R}_z(-\omega_{\mathrm{n}}t) = e^{i\omega_{\mathrm{n}}t}$:

$$\begin{aligned}\widehat{H}_{\mathrm{int}} = \hat{R}_z(-\omega_{\mathrm{n}}t)\left(\widehat{H}_0+\widehat{H}_1\right)\hat{R}_z(\omega_{\mathrm{n}}t) &= \mathrm{e}^{i\omega_{\mathrm{n}}t\hat{L}_z}\omega_{\mathrm{e}}\hat{L}_z\mathrm{e}^{-i\omega_{\mathrm{n}}t\hat{L}_z} \\ -R_0 d_{12}(\boldsymbol{R})\omega_{\mathrm{n}}\mathrm{e}^{i\omega_{\mathrm{n}}t\hat{L}_z}&\left(\mathrm{e}^{-i\omega_{\mathrm{n}}t\hat{L}_z}\hat{L}_y\mathrm{e}^{i\omega_{\mathrm{n}}t\hat{L}_z}\right)\mathrm{e}^{-i\omega_{\mathrm{n}}t\hat{L}_z} \\ &= (\omega_{\mathrm{e}}-\omega_{\mathrm{n}})\hat{L}_z - R_0 d_{12}(\boldsymbol{R})\omega_{\mathrm{n}}\hat{L}_y\end{aligned} \tag{2.27}$$

With the first term vanishing at resonance condition, this leads to a simple, time independent interaction frame Hamiltonian:

$$\widehat{H}_{\mathrm{int}} = -R_0 d_{12}(\boldsymbol{R})\omega_{\mathrm{n}}\hat{L}_y. \tag{2.28}$$

The $\widehat{H}_{\mathrm{int}}$ induces coherent population transfer between the two states, that can be described with the following two, coupled equations of motion:[8]

$$\begin{aligned} i\frac{\partial}{\partial t}\chi_1(\boldsymbol{R},t) &= \frac{1}{2}R_0 d_{12}(\boldsymbol{R})\omega_{\mathrm{n}}\chi_2(\boldsymbol{R},t) \\ i\frac{\partial}{\partial t}\chi_2(\boldsymbol{R},t) &= \frac{1}{2}R_0 d_{12}(\boldsymbol{R})\omega_{\mathrm{n}}\chi_1(\boldsymbol{R},t)\end{aligned} \tag{2.29}$$

That have the solutions[8]

$$\begin{aligned}\chi_1(\boldsymbol{R},t) &= \chi_1(\boldsymbol{R},0)\left(\cos\left(\frac{1}{2}R_0 d_{12}(\boldsymbol{R})\omega_{\mathrm{n}}t\right)\right.\\ &\quad\left.+ i\chi_2(\boldsymbol{R},0)\sin\left(\frac{1}{2}R_0 d_{12}(\boldsymbol{R})\omega_{\mathrm{n}}t\right)\right)\\ \chi_2(\boldsymbol{R},t) &= \chi_2(\boldsymbol{R},0)\left(\cos\left(\frac{1}{2}R_0 d_{12}(\boldsymbol{R})\omega_{\mathrm{n}}t\right)\right.\\ &\quad\left.+ i\chi_1(\boldsymbol{R},0)\sin\left(\frac{1}{2}R_0 d_{12}(\boldsymbol{R})\omega_{\mathrm{n}}t\right)\right)\end{aligned} \tag{2.30}$$

If we take a system, that starts at a reactant state $|r\rangle$ at t=0 with $\chi_1(\boldsymbol{R},0)=1$ and $\chi_2(\boldsymbol{R},0)=0$, population transfer takes place resulting in a full conversion to the product state $|p\rangle$ with $\chi_1(\boldsymbol{R},\tau)=0$ and $\chi_2(\boldsymbol{R},\tau)=1$ after a time

$$\tau = \frac{\pi}{R_0 d_{12}(\boldsymbol{R})\omega_{\mathrm{n}}} \tag{2.31}$$

in a semi-classical coherent interconversion process.[8]

Photoinduced processes intrinsically include transitions between and interactions of different adiabatic states. Equations 2.30 give a straightforward description of coherent charge transfer between two adiabatic electronic states coupled to a single, long lived nuclear mode, giving deep insight into the role of electronic coherence, nuclear-electronic resonance, converging time scales of electronic and nuclear motion as well as the role of symmetry. Furthermore, due to the relaxation from the Franck-Condon region, an excited molecular system sweeps through resonance, which makes ω_{e} as well as d_{12} time dependent, contrary to this pseudo static approach that considers the system at the exact resonance. To model transitions between adiabatic states in complex molecular systems, the Schrödinger equation of the molecular problem given in equation 2.14 should therefore be the starting point. The non-adiabatic coupling terms need to be included to allow for transitions between adiabatic states. Several approaches of non-adiabatic molecular dynamics (NAMD) will be explained in section 2.5, while an in-depth investigation of vibronic coupling and coherence in intermolecular charge transfer is the main focus of chapter 3.

2.2 Density Functional Theory

Density Functional Theory (DFT) has proven to be the workhorse of modern computational chemistry. The main reason for its relatively low computational cost is the description of the electronic system not in terms of 4*n*-dimensional wavefunctions (3 spatial coordinates and 1 spin variable per electron), but rather an electron density dependent only on the 3 spatial coordinates. This is done on the basis of the first Hohenberg-Kohn theorem,[3] which states that a one-on-one mapping between electronic wavefunction, external potential and electron density exists,

$$\rho(\boldsymbol{r}) \leftrightarrow \hat{V}_{ext} \leftrightarrow \psi(\boldsymbol{r}) \tag{2.32}$$

so that an electron density can uniquely be assigned to a many-electron wavefunction and an external potential for any given system, and vice versa. The external potential includes the electron-nuclei interaction and can in principle also include further contributions. Since all observables of the system are a functional of the wavefunction, they can therefore also be described by a functional of the electron density, for example for the energy of the system:

$$\begin{aligned} E[\psi(\boldsymbol{r})] = \int_{\Omega_{\mathrm{tot}}} d\boldsymbol{r}\, \psi^*(\boldsymbol{r})\big(\hat{T}_{\mathrm{el}} + \hat{V}_{\mathrm{el,el}} + \hat{V}_{\mathrm{ext}}\big)\psi(\boldsymbol{r}) \leftrightarrow \\ E[\rho(\boldsymbol{r})] = T_{\mathrm{el}}[\rho(\boldsymbol{r})] + V_{\mathrm{el,el}}[\rho(\boldsymbol{r})] + V_{\mathrm{ext}}[\rho(\boldsymbol{r})] \\ = HK[\rho(\boldsymbol{r})] + V_{\mathrm{ext}}[\rho(\boldsymbol{r})] \end{aligned} \tag{2.33}$$

with $HK[\rho(\boldsymbol{r})] = T_{\mathrm{el}}[\rho(\boldsymbol{r})] + V_{\mathrm{el,el}}[\rho(\boldsymbol{r})]$ the Hohenberg-Kohn functional. The functional for the nuclei-nuclei interaction is not included since this is a constant term within the BOA and can be added to the energy at a later stage. The ground state energy can be found by using the second Hohenberg-Kohn theorem, which states that the ground state electron density $\rho_0(\boldsymbol{r})$ minimizes the energy functional.

$$E_0 = E[\,\rho_0(\boldsymbol{r})] \leq E[\rho] \tag{2.34}$$

This means that the variational principle can be used to optimize the electron density to yield the lowest possible energy. In practice however, the form of the exact Hohenberg-Kohn Functional is unfortunately not known. The problem here are the kinetic energy functional for the electrons and the electron-electron interaction, that are both unknown for interacting electrons. To circumvent this problem, Kohn and Sham postulated that for each system of interacting electrons at a certain external potential and corresponding electron density, a hypothetical system (a 'Kohn-Sham system') of non-interacting electrons with the same electron density can be found moving in an effective potential $v_{\mathrm{eff}}(\boldsymbol{r})$.[10] The electron density of the non-interacting system is build up by Kohn-Sham orbitals $\phi_i(\boldsymbol{r})$

$$\rho_{\mathrm{eff}}(\boldsymbol{r}) = \sum_{i}^{n} |\phi_i(\boldsymbol{r})|^2 \tag{2.35}$$

that are found by solving *n* coupled equations for the lowest possible energy:

$$\left(-\frac{1}{2}\nabla^2 + v_{\mathrm{eff}}(\boldsymbol{r})\right)\phi_i(\boldsymbol{r}) = \varepsilon_i \phi_i(\boldsymbol{r}) \tag{2.36}$$

With the use of the Kohn-Sham orbitals, the energy functional can be decomposed in several large known contributions and possibly smaller unknown terms that need to be approximated: The kinetic energy functional can be split into one functional for non-interacting electrons by using the non-interacting kinetic energy functional $T_{\mathrm{eff}}[\rho(\boldsymbol{r})]$ and an unknown kinetic correlation energy term $T_{\mathrm{corr}}[\rho(\boldsymbol{r})]$. The electron-electron interaction can also be split into a pure Coulomb interaction term $J[\rho(\boldsymbol{r})]$ and a non-classical unknown part $V_{\mathrm{nc}}[\rho(\boldsymbol{r})]$. The two unknown funtionals are combined into the exchange correlation functional $E_{\mathrm{XC}}[\rho(\boldsymbol{r})] = T_{\mathrm{corr}}[\rho(\boldsymbol{r})] + V_{\mathrm{nc}}[\rho(\boldsymbol{r})]$, and we get for the total energy functional:

$$E[\rho(\boldsymbol{r})] = T_{\mathrm{eff}}[\rho(\boldsymbol{r})] + J[\rho(\boldsymbol{r})] + V_{\mathrm{ext}}[\rho(\boldsymbol{r})] + E_{\mathrm{XC}}[\rho(\boldsymbol{r})] \tag{2.37}$$

Variational optimization of this functional with respect to the Kohn-Sham orbitals subject to the orthonormality constraint leads to the Kohn-Sham equations that need to be self-consistently solved:

$$\left(-\frac{\nabla^2}{2}+\int_{\Omega_{\mathrm{tot}}} d\boldsymbol{r}'\,\frac{\rho(\boldsymbol{r}')}{|\boldsymbol{r}-\boldsymbol{r}'|}+v_{\mathrm{ext}}(\boldsymbol{r})+\varepsilon_{\mathrm{XC}}(\boldsymbol{r})\right)\phi_i(\boldsymbol{r})=\varepsilon_i\phi_i(\boldsymbol{r}) \tag{2.38}$$

The term $\varepsilon_{\mathrm{XC}}$ is the functional derivative with respect to the electron density of the exchange correlation term.

For the exchange correlation (XC) functional, there are numerous approximations to be found.[11] Within the Local Density Approximation (LDA),[10] the XC-functional is based on the known exchange correlation energy of a homogeneous electron gas (HEG):

$$E_{\mathrm{XC}}^{\mathrm{LDA}}[\rho(\boldsymbol{r})]=\int_{\Omega_{\mathrm{tot}}} d\boldsymbol{r}\,\varepsilon_{\mathrm{XC}}^{\mathrm{HEG}}\big(\rho(\boldsymbol{r})\big)\rho(\boldsymbol{r}) \tag{2.39}$$

LDA gives quite good results in systems of relatively uniform electron density distributions such as extended metal systems or semi-conductors. In systems of abrupt electron density changes such as organic molecules, it is not as reliable and instead, XC-functionals of the GGA (Generalized Gradient Approximation) family are used, where the gradient of the electron density is also taken into account:

$$\begin{aligned}E_{\mathrm{XC}}^{\mathrm{GGA}}[\rho(\boldsymbol{r})]=&\int_{\Omega_{\mathrm{tot}}} d\boldsymbol{r}\,\varepsilon_{\mathrm{XC}}^{\mathrm{HEG}}\big(\rho(\boldsymbol{r})\big)\rho(\boldsymbol{r})\\&+\int_{\Omega_{\mathrm{tot}}} d\boldsymbol{r}\,F_{\mathrm{XC}}[\rho(\boldsymbol{r}),\nabla\rho(\boldsymbol{r})]\rho(\boldsymbol{r})\end{aligned} \tag{2.40}$$

with $F_{\mathrm{XC}}[\rho(\boldsymbol{r}),\nabla\rho(\boldsymbol{r})]$ depending on both the electron density as well as its gradient. Examples of this family are the functionals called BLYP and PBE that are also used in this work.[12–15]

Another set of XC-functionals quite commonly used are hybrid functionals, that include a fraction of exact Hartree-Fock exchange energy. One example used in this work is the extensively used B3LYP functional.[13,16]

The choice of the XC-functional is quite crucial in describing chemical systems accurately and is highly dependent on the specific system and on the molecular properties of interest.

Linear Response Time Dependent DFT

DFT is strictly a ground state approach, describing a system in its unperturbed stable state. To model interactions with electromagnetic irradiation which perturbs the system, Runge and Gross introduced a theorem that states that for each system that evolves in a time dependent external potential $\hat{V}_{ext}(t)$, there exists a direct mapping to a time dependent electron density $\rho(\boldsymbol{r},t)$ and time dependent wave function :[4]

$$\rho(\boldsymbol{r},t) \leftrightarrow \hat{V}_{\text{ext}}(t) \leftrightarrow \psi(\boldsymbol{r},t) \tag{2.41}$$

Parallel to ground state DFT, the system can be described by non-interacting Kohn-Sham orbitals, leading to the time-dependent Kohn-Sham equations:

$$\left(-\frac{\nabla^2}{2} + \int_{\Omega_{\text{tot}}} d\boldsymbol{r}' \frac{\rho(\boldsymbol{r}',t)}{|\boldsymbol{r}-\boldsymbol{r}'|} + v_{\text{ext}}(\boldsymbol{r},t) + \varepsilon_{\text{XC}}(\boldsymbol{r},t)\right)\phi_i(\boldsymbol{r}) = i\frac{\partial}{\partial t}\phi_i(\boldsymbol{r}) \tag{2.42}$$

In Linear Response Time Dependent DFT (LR-TDDFT), the time-dependency of the electronic system is treated as the response of a ground state density $\rho_{t_0}(\boldsymbol{r})$ at time t_0 to a perturbation of frequency ω introduced through the external potential at $t>t_0$, so that

$$v_{\text{ext}}(\boldsymbol{r},\omega) = v_{t_0}^{\text{ext}}(\boldsymbol{r}) + \delta v_{\text{ext}}(\boldsymbol{r},\omega)$$
$$\rho(\boldsymbol{r},\omega) = \rho_{t_0}(\boldsymbol{r}) + \delta\rho(\boldsymbol{r},\omega) \tag{2.43}$$

This perturbation can be represented as a Taylor series. In LR-TDDFT, only the first order term, the linear response is considered. Furthermore, the response of the electron density to the external potential can again be described by a system of non-

interacting electrons responding to an effective external potential v_{eff}. The first order response in the electron density becomes

$$\delta\rho(\boldsymbol{r},\omega) = \int_{\Omega_{\text{tot}}} d\boldsymbol{r}'\,\chi(\boldsymbol{r},\boldsymbol{r}';\boldsymbol{\omega})\delta v_{\text{eff}}(\boldsymbol{r}',\omega) \tag{2.44}$$

with $\chi(\boldsymbol{r},\boldsymbol{r}';\boldsymbol{\omega})$ being called the response function, which for the non-interacting system takes the form

$$\chi(\boldsymbol{r},\boldsymbol{r}';\boldsymbol{\omega}) = \sum_{i=1}^{occ}\sum_{k=1}^{virt} 2\frac{\omega_{ki}}{\omega^2-\omega_{ki}^2}\phi_i(\boldsymbol{r})\phi_k(\boldsymbol{r})\phi_i(\boldsymbol{r}')\phi_k(\boldsymbol{r}') \tag{2.45}$$

with ϕ_{i} the occupied Kohn-Sham orbitals and ϕ_{k} the virtual and their energy difference determining $\omega_{ki} = \varepsilon_k - \varepsilon_i$. The response function displays singularities at the excitation energies.

The perturbation of the effective potential $\delta v_{\text{eff}}(\boldsymbol{r}',\omega)$ contains the change in the external potential $\delta v_{\text{ext}}(\boldsymbol{r},\omega)$ and electron density $\delta\rho(\boldsymbol{r}',\omega)$:

$$\delta v_{\text{eff}}(\boldsymbol{r}',\omega) = \delta v_{\text{ext}}(\boldsymbol{r},\omega) + \int_{\Omega_{\text{tot}}} d\boldsymbol{r}'\frac{\delta\rho(\boldsymbol{r}',\omega)}{|\boldsymbol{r}-\boldsymbol{r}'|} + \int_{\Omega_{\text{tot}}} d\boldsymbol{r}'\,f_{\text{xc}}(\boldsymbol{r},\boldsymbol{r}';\omega)\,\delta\rho(\boldsymbol{r},\omega) \tag{2.46}$$

with $f_{\text{xc}}(\boldsymbol{r},\boldsymbol{r}';\omega)$ the time dependent exchange correlation kernel, whose exact form, as the XC-Functionals, is not known and needs to be approximated. In this work, the standard ALDA (Adiabatic LDA) kernel is employed in all linear response TD-DFT calculations.

From LR-TTDFT it is possible to get relatively reliable excitation energies. However, Charge Transfer (CT) excitations are poorly described due to the long-range interactions not well described in most XC-functionals. To overcome this, a class of Long range Corrected (LC) functionals have been introduced, including the here used CAMY-B3LYP functional.[13,16–18].

2.3 Semi-Empirical Tight Binding Methods

Even though DFT is a cheap method in comparison to more elaborate wave function-based methods, it also becomes very expensive in extended systems. To describe such large systems, semi-empirical methods can be a great compromise between accuracy and computational cost. Traditional semi-empirical methods start from the Hartree-Fock approximation, but introduce simplifications in the Hamiltonian matrix and replace remaining terms with empirical parameters, which are used to include approximate correlation effects. One of the earliest of these methods was developed by Erich Hückel in the 1930s and today bears his name.[19–22]

Hückel Theory and Extended Hückel Theory

The original Hückel theory simplified the quantum mechanical description of planar hydrocarbons with extended conjugated π-systems to such an extent, that it was possible to obtain energies of π-systems and explain aromaticity on a quantum mechanical level in a time when computational tools for solving quantum mechanical problems were unavailable. The main approximation is that the electronic and energetic properties of this class of molecules are almost entirely dictated by the conjugated π-orbitals. The original Hückel method therefore disregarded sigma orbitals entirely and only took π-orbitals into consideration. The Extended Hückel (EH) theory introduced by Roald Hoffmann in 1963, expanded the description to all valence electrons, thus also including σ-orbitals.[23] The total wavefunction is described as a product of *n* one-electron wavefunctions $\psi_j(\boldsymbol{r_j})$, with *n* being the number of valence electrons, that are in turn constructed by a linear combination of *N* atomic orbitals.

$$\Psi_{tot} = \psi_1(\boldsymbol{r}_1)\psi_2(\boldsymbol{r}_2) \ldots . \psi_n(\boldsymbol{r_n}) \tag{2.47}$$

$$\psi_j = \sum_{i=1}^{N} a_{ij}\varphi_i \tag{2.48}$$

The atomic orbitals φ_i are Slater Type Orbitals (STOs). Here, since the basis set is minimal, $N=n$. The total energy of the system can then be determined by the sum of the single electron energies ε_j, which in turn are obtained by solving

$$\hat{h}_{\text{eff}}\psi_j = \varepsilon_j\psi_j \tag{2.49}$$

with $\hat{h}_{\text{eff}}$ a single electron Hamiltonian that includes effective interactions with the other particles. These n one-electron equations can be rewritten in the form of n secular equations:

$$\begin{aligned} a_{i1}(H_{i1} - ES_{i1}) + (H_{i2} - ES_{i2}) + \cdots + a_{im}(H_{im} - ES_{im}) \\ + a_{iN}(H_{iN} - ES_{iN}) = 0 \end{aligned} \tag{2.50}$$

with E the energy, H_{ii} the Coulomb Integrals,

$$H_{ii} = \langle\varphi_i|\hat{h}_{\text{eff}}|\varphi_i\rangle, \tag{2.51}$$

H_{im} the Resonance Integrals

$$H_{im} = \langle\varphi_i|\hat{h}_{\text{eff}}|\varphi_m\rangle \tag{2.52}$$

and S_{im} Overlap Integrals

$$S_{im} = \langle\varphi_i|\varphi_m\rangle. \tag{2.53}$$

With the secular determinant

$$\begin{vmatrix} H_{11} - ES_{11} & H_{12} - ES_{12} & \cdots & H_{1m} - ES_{1m} & \cdots & H_{1N} - ES_{1N} \\ H_{21} - ES_{21} & H_{22} - ES_{22} & \cdots & H_{2m} - ES_{2m} & \cdots & H_{2N} - ES_{2N} \\ \vdots & \vdots & \ddots & \vdots & \ddots & \vdots \\ H_{i1} - ES_{i1} & H_{i2} - ES_{i2} & \cdots & H_{im} - ES_{im} & \cdots & H_{iN} - ES_{iN} \\ \vdots & \vdots & \ddots & \vdots & \ddots & \vdots \\ H_{N1} - ES_{N1} & H_{N2} - ES_{N2} & \cdots & H_{Nm} - ES_{Nm} & \cdots & H_{NN} - ES_{NN} \end{vmatrix} = 0 \tag{2.54}$$

the orbital energies, and then the orbital coefficients can be determined.

The most relevant approximation of EH, that makes it especially cost effective, is to parametrize these integrals instead of using their explicit description. Therefore, the exact expression of $\hat{h}_{\text{eff}}$ does not need to be known within the EH method. The diagonal terms of the matrix are readily evaluated: the overlap integrals S_{ii} are 1, as this is the spatial overlap between the atomic orbital φ_i with itself. The term H_{ii} is the Coulomb integral, an optimized parameter describing the kinetic and potential energy of an electron in orbital φ_i, most often described in terms of the negative of the orbital ionization potential. The off-diagonal elements include both the overlap integrals S_{im} and the Resonance Integrals H_{im}. Since the form and position of the atomic orbitals are known, S_{im} can be determined from the interatomic distances. The Resonance Integrals, describing the interaction of the electrons in orbital φ_i and φ_m are evaluated as:

$$H_{im} = \frac{1}{2} k_{im}(H_{ii} + H_{mm})S_{im}. \tag{2.55}$$

Here, k_{im} is an empirical parameter, called the Wolfsberg-Helmholz parameter. To obtain reliable energies, the EH parameters H_{ii}, k_{im} and the effective nuclear charges ζ that are embedded in the STOs are then optimized so that EH reproduces experimental or higher-level theoretical results. With that approach, the EH method can be used to obtain extremely cheap descriptions of both the electronic structure and the electronic energies. Molecular structures are not very reliable due to the non-self-consistent nature of EH, which is why this method is often used in combination with structures and trajectories of higher-level methods (even other tight binding methods as described in chapter 4 and 6).

Density Functional Based Tight Binding

A rather successfully employed semi-empirical approach, parametrized on DFT results rather than experimental data, is the Density Functional based Tight Binding (DFTB) method.[24,25] For DFTB the general expression of the energy is

$$E_{\mathrm{DFTB}} = \sum_{j}^{\mathrm{occ}} \langle \psi_j | \hat{H}_0 | \psi_j \rangle + E_{\mathrm{rep}}, \tag{2.56}$$

with $\hat{H}_0 = \hat{T}_{\mathrm{el}} + V_{\mathrm{eff}}(\boldsymbol{r})$ the unperturbed zero-order Hamiltonian. The effective potential $V_{\mathrm{eff}}(\boldsymbol{r})$ is approximated as a summation of purely atomic contributions, ψ_j the molecular orbitals, and the E_{rep} the atom-pair short range repulsion discussed later.

The molecular orbitals are expanded in STO's, similar to the EH approach in equation 2.48. The first term including the molecular orbital energies can be determined as in EH by solving the secular determinant (equation 2.54). Parametrization of the Coulomb and Resonance integrals however is done differently. The Coulomb Integral H_{ii} is determined by an LDA calculation of a free neutral pseudoatom according to

$$H_{ii} = \varepsilon_i^{\text{neutral free atom}}. \tag{2.57}$$

The resonance integrals are assumed to be 0 for the case that the orbitals in question reside on the same atom, otherwise, they are estimated by

$$H_{ij} = \langle \varphi_i^A | \hat{T}_{\mathrm{el}} + \hat{V}^A + \hat{V}^B | \varphi_j^B \rangle. \tag{2.58}$$

In equation 2.58 the potential operators for atoms *A* and *B* are included by strictly pairwise contributions of only two-center terms.

By solving the secular equations, the first term in equation 2.56 becomes a summation over all occupied Kohn-Sham orbitals with energy ε_j and occupation number n_j. The short range repulsion part E_{rep} is then taken as a function dependent

on distance R_{AB} and is determined by the difference of an LDA reference energy and the corresponding DFTB energy determined for reference structures of A and B

$$E_{\mathrm{rep}}(R_{AB}) = \left[E_{\mathrm{LDA}}(R_{AB}) - \sum_{j}^{\mathrm{occ}} n_j \varepsilon_j(R_{AB}) \right]_{\text{reference structure}} \tag{2.59}$$

For the practical implementation and application, a DFTB based program requires atomic parameters for each involved element including *e.g.* the STO atomic orbitals and Coulomb integral, and also pairwise parameters of each possible combination of two elements for the short range repulsion term.

The disadvantage of this tight binding approach is the negligence of long-range interactions. One extension that includes long-range Coulomb interactions is the Self-Consistent-Charge variant of DFTB, SCC-DFTB.[26–28] In this case, equation 2.56 includes an additional term

$$E_{\mathrm{DFTB}} = \sum_{j=1}^{\mathrm{occ}} \langle \Psi_j | \widehat{H}_0 | \Psi_j \rangle + \frac{1}{2} \sum_{A,B}^{N} q_A q_B \gamma_{AB} + E_{\mathrm{rep}} \tag{2.60}$$

describing long-range Coulomb interactions between atoms *A* and *B* with point charges q_A and q_B, with γ_{AB} being a shorthand notation for

$$\gamma_{AB} = \frac{1}{\boldsymbol{R}_{AB}} - S(U_A, U_B, \boldsymbol{R}_{AB}). \tag{2.61}$$

$S(U_A, U_B, \boldsymbol{R}_{AB})$ is a short-range correction function that decays exponentially and is a function of the distance $\boldsymbol{R}_{AB}$ between atoms *A* and *B* and U_A, U_B are element specific Hubbard parameters of *A* and *B*.[27]

Even though the first term and the third term in equation 2.60 are the same as for canonical DFTB, the dependence of the atomic charges on the electron density and its influence on the total energy results in a self-consistent approach regarding the energy minimization.

Geometry, Frequency, Noncovalent, eXtended Tight Binding

A further development in semi-empirical methods is the GFN-xTB method developed by the Grimme group in Bonn.[29] GFN-xTB stands for Geometry, Frequency, Noncovalent, eXtended Tight Binding and as the name denotes has been optimized to accurately describe the structural properties of chemical compounds. There are no atom-pair based parameters but only global and element specific parameters, which makes GFN-xTB an extremely applicable method over a diverse range of chemical systems. The basis consists, similar to DFTB and the extended Hückel method, of a minimal basis set of STOs. Additionally, s-functions for hydrogen are augmented to improve description of hydrogen bonding, while the d-orbitals include polarization functions.

The total energy of a chemical system determined by GFN-xTB in atomic units contains the following energy terms:

$$E_{\mathrm{GFN-xTB}} = E_{\mathrm{el}} + E_{\mathrm{rep}} + E_{\mathrm{disp}} + E_{\mathrm{XB}} \tag{2.62}$$

The electronic energy term E_{el}, the repulsion energy term E_{rep} for atom-pair repulsion, the dispersion energy term E_{disp} and the E_{XB} term that includes halogen bonding effects. The atom-pair repulsion between atoms A and B with effective nuclear charges Z^{eff} and a distance R_{AB} is represented as

$$E_{\mathrm{rep}} = \sum_{A,B}^{N} \frac{Z_A^{\mathrm{eff}} Z_B^{\mathrm{eff}}}{R_{AB}} e^{-\sqrt{\alpha_A \alpha_B} R_{AB}{}^{k_{\mathrm{f}}}} \tag{2.63}$$

with α being a scaling parameter optimized for each element, while k_{f} is a global parameter with a value of 1.5[29]. The dispersion energy is determined by the common D3 dispersion corrections with BJ-damping functions.[30,31]

The halogen bonding term is described through a modified Lennard-Jones potential. Since it bears no relevance for this work, as no halogen atoms were used in any of the systems, it is not included here. A full description can be found in reference [29].

The electronic energy term is quite similar to equation 2.56 for SCC-DFTB:

$$E_{\mathrm{el}} = \sum_{i=1}^{\mathrm{occ}} n_i \langle \psi_i | \widehat{H}_0 | \psi_i \rangle + \frac{1}{2} \sum_{A,B}^{N} \sum_{l(A)}^{n_{l(A)}} \sum_{l'(B)}^{n_{l'(B)}} p_l^A p_{l'}^B \gamma_{AB,ll'} + \frac{1}{3} \sum_{A=1}^{N} \Gamma_A q_A^3 - T_{\mathrm{el}} S_{\mathrm{el}} \tag{2.64}$$

with the first term giving the orbital energies of the occupied orbitals ψ_i (as explained in the DFTB section) given their population n_i, and the zero-order unperturbed Hamiltonian $\widehat{H}_0$. The second term, similar in SCC-DFTB, includes the long-range Coulomb interaction between atoms *A* and *B* of a distance R_{AB}. The summation goes over all atomic shells of atom *A* (*l*) and atom *B* (*l'*), with p_l^A denoting the charge distribution of atom *A* and shell *l*. γ_{AB} is here given by

$$\gamma_{AB} = \left(\frac{1}{R_{AB}^{k_g} + \eta^{-k_g}} \right)^{1/k_g} \tag{2.65}$$

with $k_g = 2.0$ a global parameter[29] and

$$\eta = 2 \left(\frac{1}{(1 + \kappa_A^l)\eta_A} + \frac{1}{(1 + \kappa_B^{l'})\eta_B} \right)^{-1} \tag{2.66}$$

where κ_A^l and $\kappa_B^{l'}$ are scaling factors that are, as the chemical hardness η_A and η_B element specific parameters.

In the third term, q_A is the point charge of atom *A*, while Γ_A is the charge derivative of the atomic Hubbard parameter. These are the diagonal terms of the third-order density fluctuations. The last term is the electronic entropy, that becomes relevant in open shell systems with fractional occupations.

2.4 Adiabatic *Ab Initio* Molecular Dynamics

In general, adiabatic nuclear dynamics should be performed following equation 2.15, where the nuclei are propagated on an adiabatic PES generated by the electronic system at nuclear positions $\boldsymbol{R}$. However, as nuclei are rather heavy particles, it is often assumed that they behave as classical particles. The movement of the nuclei over time can then be described by Newton's second law of motion:

$$m_I \frac{d^2 \boldsymbol{R}_I(t)}{dt^2} = F(\boldsymbol{R}_I(t)) = -\nabla V_{\mathrm{el}}(\boldsymbol{R}_I(t)) \tag{2.67}$$

where the Force $F(\boldsymbol{R}_I)$ is determined by the electronic system through the nuclear coordinate dependent $V_{\mathrm{el}}(\boldsymbol{R}_I)$. In classical MD, this potential and with it the entire influence of the electronic system is collapsed into parametrized force fields, describing bonded interactions as covalent bond distances, angles, dihedrals, as well as non-bonded interactions by model potentials. However, these modelled interactions, often following the harmonic approximation for bonded interactions, are a stark simplification of the electronic influence on the nuclear dynamics. To describe chemical reactions, involving breaking and forming of covalent bonds, classical force fields fall short and non-harmonic potentials are necessary, for example in the framework of reactive force fields.[32] However, these electronic potentials can also be determined using quantum mechanical electronic structure methods, by using the classical limit of equation 2.15:

$$\begin{aligned} m_I \frac{d^2 \boldsymbol{R}_I(t)}{dt^2} &= -\nabla \left\langle \psi_0\left(\boldsymbol{r}; \boldsymbol{R}_I(t)\right) \middle| \widehat{H}_{\mathrm{el}} \middle| \psi_0\left(\boldsymbol{r}; \boldsymbol{R}_I(t)\right) \right\rangle \\ &= -\nabla V_{\mathrm{el}}^0(\boldsymbol{R}_I(t)) \end{aligned} \tag{2.68}$$

The classical nuclei are evolved on a potential determined by the ground state energy of the electronic quantum system, which corresponds to the multidimensional potential energy surface of the ground state. This PES is normally calculated on the fly, with new nuclear coordinates at time *t* determining the electronic Hamiltonian and by solving the time independent Schrödinger equation for the electronic system (see equation 2.04) using the electronic structure method of choice. The gradient of

the electronic energy calculated on that point determines the forces acting on the nuclei. The forces lead to a modified nuclear geometry, that defines an updated electronic Hamiltonian. This quantum-classical method is also called Born-Oppenheimer Molecular Dynamics (BOMD). In general, the system can also be evolved in a state that is different from the ground state, using *e.g.* LR-TDDFT as the electronic structure method; however, due to the adiabatic BOA and static treatment of the electrons, non-adiabatic effects such as transitions between adiabatic states cannot be simulated.

2.5 Nonadiabatic Molecular Dynamics (NAMD)

While AIMD methods are a powerful tool to simulate chemical reactions, photochemistry is inherently non-adiabatic. Photochemical reactions therefore need to be treated with methods that allow for non-adiabatic transitions. To allow for these transitions, the electronic system needs to be treated explicitly time dependent. Usually, the time dependent electronic wavefunction is written as a linear combination of adiabatic electronic wave functions with time dependent coefficients $c_i(t)$:

$$\psi(\boldsymbol{r}, t) = \sum_{i=1}^{\infty} c_i(t)\psi_i(\boldsymbol{r}; \boldsymbol{R}(t)) \tag{2.69}$$

The direct time dependence is only in the coefficients, while the adiabatic wave functions are only indirectly dependent on time through the parametric dependence on the nuclear coordinates. The time dependent Schrödinger equation for the electrons then becomes:

$$i\sum_{i=1}^{\infty} \frac{\partial(c_i(t)\psi_i(\boldsymbol{r}; \boldsymbol{R}(t)))}{\partial t} = \hat{H}_{\mathrm{el}} \sum_{i=1}^{\infty} c_i(t)\psi_i(\boldsymbol{r}; \boldsymbol{R}(t)) \tag{2.70}$$

Multiplying with the complex conjugate ψ_j^* and integrating over $\boldsymbol{r}$, as in equation 2.07, gives

$$i\sum_{i=1}^{\infty}\frac{\partial c_i(t)\delta_{ij}}{\partial t}+i\int_{\Omega_{\mathrm{tot}}}d\boldsymbol{r}\psi_j^*(\boldsymbol{r};\boldsymbol{R}(t))\sum_{i=1}^{\infty}c_i(t)\frac{\partial\psi_i(\boldsymbol{r};\boldsymbol{R}(t))}{\partial t}$$

$$=\int_{\Omega_{\mathrm{tot}}}d\boldsymbol{r}\psi_j^*(\boldsymbol{r};\boldsymbol{R}(t))\widehat{H}_{\mathrm{el}}\sum_{i=1}^{\infty}c_i(t)\psi_i(\boldsymbol{r};\boldsymbol{R}(t)) \tag{2.71}$$

Rearranging and using equation 2.13 as well as the chain rule, we get the following coupled differential equations:

$$i\frac{\partial c_j(t)}{\partial t}=\sum_{i=1}^{\infty}c_i(t)\left[H_{ji}\big(\boldsymbol{R}(t)\big)-i\boldsymbol{d}_{ji}(\boldsymbol{R}(t))\frac{d\boldsymbol{R}(t)}{dt}\right] \tag{2.72}$$

With the Hamiltonian matrix

$$H_{ji}\big(\boldsymbol{R}(t)\big)=\int_{\Omega_{\mathrm{tot}}}d\boldsymbol{r}\;\psi_j^*(\boldsymbol{r};\boldsymbol{R}(t))\widehat{H}_{\mathrm{el}}\psi_i(\boldsymbol{r};\boldsymbol{R}(t)) \tag{2.73}$$

Equation 2.72 determines the time evolution of the coefficients of the adiabatic states. It is important to note, that the coefficient of state *j* depends on all other adiabatic states *i*. Both $H_{ji}\big(\boldsymbol{R}(t)\big)$ as well as $\boldsymbol{d}_{ji}(\boldsymbol{R}(t))$ allow for interaction of different adiabatic states. Both are parametrically dependent on $\boldsymbol{R}(t)$, showing the importance of the nuclear motion in the transition process. The non-adiabatic coupling vector $\boldsymbol{d}_{ji}(\boldsymbol{R}(t))$ allows for transitions from one adiabatic state to another in regions of strong coupling. The off-diagonal matrix elements of the Hamiltonian couple different states and are important in the diabatic representation or for non-orthonormal functions; they become however 0 when using an orthonormal, time independent adiabatic basis as done here. Thus, the equations for the time evolution of the coefficients becomes[33]

$$i\frac{\partial c_j(t)}{\partial t}=c_j(t)\varepsilon_i(\boldsymbol{R}(t))-i\sum_{i=1}^{\infty}\boldsymbol{d}_{ji}(\boldsymbol{R}(t))\frac{d\boldsymbol{R}}{dt} \tag{2.74}$$

The two NAMD methods used in this work differ in both the exact time evolution of the coefficients as given in equation 2.74 as well as in the time evolution of the nuclei.

Ehrenfest Dynamics

Ehrenfest dynamics is a quantum-classical mean field approach to NAMD. As in adiabatic AIMD, the nuclei are assumed to be classical particles and evolve according to forces determined quantum mechanically:[33–35]

$$m_I \frac{d^2 \boldsymbol{R}_I(t)}{dt^2} = -\nabla \left\langle \psi(\boldsymbol{r}, t; \boldsymbol{R}_I(t)) \middle| \widehat{H}_{\mathrm{el}} \middle| \psi(\boldsymbol{r}, t; \boldsymbol{R}_I(t)) \right\rangle \tag{2.75}$$

Differently to equation 2.68, equation 2.75 does not necessarily involve the adiabatic ground state electronic wavefunction and retains the explicit time dependence of $\psi(\boldsymbol{r}, t; \boldsymbol{R}_I)$. Still, this equation shows the single configuration character of Ehrenfest dynamics, where the nuclei are evolved according to a mean potential as opposed to a multi-configuration based method as Multi Configurational Time dependent Hartree (MCTDH), which allows for propagation on different states and branching of the wave function.[36,37] The forces can be determined using the Hellmann-Feynman theorem:

$$F_I = -\left\langle \psi(\boldsymbol{r}, t; \boldsymbol{R}_I(t)) \middle| \nabla_I \widehat{H}_{\mathrm{el}} \middle| \psi(\boldsymbol{r}, t; \boldsymbol{R}_I(t)) \right\rangle \tag{2.76}$$

Again, using time independent adiabatic basis functions with time dependent coefficients, inserting equation 2.69 into equation 2.76, we get

$$F_I = -\sum_{i,j}^{\infty} \left\langle c_j(t)\psi_j(\boldsymbol{r}; \boldsymbol{R}_I(t)) \middle| \nabla_I \widehat{H}_{\mathrm{el}} \middle| c_i(t)\psi_i(\boldsymbol{r}; \boldsymbol{R}_I(t)) \right\rangle \tag{2.77}$$

Noting that

$$\nabla_I \left\langle c_j(t)\psi_j(\boldsymbol{r}; \boldsymbol{R}_I(t)) \middle| \widehat{H}_{\mathrm{el}} \middle| c_i(t)\psi_i(\boldsymbol{r}; \boldsymbol{R}_I(t)) \right\rangle = \nabla_I c_j^* c_i \varepsilon_j \delta_{ji} \tag{2.78}$$

and

$$\begin{aligned}
&\nabla_I \left\langle c_j(t)\psi_j(\boldsymbol{r};\boldsymbol{R}_I(t)) \middle| \widehat{H}_{\mathrm{el}} \middle| c_i(t)\psi_i(\boldsymbol{r};\boldsymbol{R}_I(t)) \right\rangle \\
&\quad = \left\langle \nabla_I c_j(t)\psi_j(\boldsymbol{r};\boldsymbol{R}_I(t)) \middle| \widehat{H}_{el} \middle| c_i(t)\psi_i(\boldsymbol{r};\boldsymbol{R}_I(t)) \right\rangle \\
&\quad + \left\langle c_j(t)\psi_j(\boldsymbol{r};\boldsymbol{R}_I(t)) \middle| \nabla_I \widehat{H}_{\mathrm{el}} \middle| c_i(t)\psi_i(\boldsymbol{r};\boldsymbol{R}_I(t)) \right\rangle \\
&\quad + \left\langle c_j(t)\psi_j(\boldsymbol{r};\boldsymbol{R}_I(t)) \middle| \widehat{H}_{\mathrm{el}} \middle| \nabla_I c_i(t)\psi_i(\boldsymbol{r};\boldsymbol{R}_I(t)) \right\rangle \\
&\quad = \left\langle c_j(t)\psi_j(\boldsymbol{r};\boldsymbol{R}_I(t)) \middle| \nabla_I \widehat{H}_{\mathrm{el}} \middle| c_i(t)\psi_i(\boldsymbol{r};\boldsymbol{R}_I(t)) \right\rangle \\
&\quad + c_j^* c_i (\varepsilon_j - \varepsilon_i)\boldsymbol{d}_{ji}
\end{aligned} \tag{2.79}$$

where we used that both operators are Hermitian and $-\boldsymbol{d}_{ij} = \boldsymbol{d}_{ji}$, we get

$$\begin{aligned}
&\left\langle c_j(t)\psi_j(\boldsymbol{r};\boldsymbol{R}_I(t)) \middle| \nabla_I \widehat{H}_{\mathrm{el}} \middle| c_i(t)\psi_i(\boldsymbol{r};\boldsymbol{R}_I(t)) \right\rangle \\
&\quad = \nabla_I c_j^* c_i \varepsilon_j \delta_{ji} - c_j^* c_i (\varepsilon_j - \varepsilon_i)\boldsymbol{d}_{ji}
\end{aligned} \tag{2.80}$$

Finally inserting into equation 2.76, we obtain the forces for the nuclei:[33]

$$F_I = -\sum_{j=1}^{\infty} |c_j|^2 \varepsilon_j + \sum_{j\neq i}^{\infty} c_j^* c_i (\varepsilon_j - \varepsilon_i)\boldsymbol{d}_{ji} \tag{2.81}$$

Therefore, the nuclei evolve on a mean potential, determined by the populations of different, mixed adiabatic states. The last term is the influence of non-adiabatic transitions between different states on the forces acting on the nuclei, that contains the non-adiabatic coupling vector $\boldsymbol{d}_{ji}$.The electronic motion is described following equation 2.74. Both subsystems are therefore coupled to each other: the nuclei move on a potential that is dependent on the average potential determined by the populations of the different adiabatic electronic states, while the electronic subsystem is coupled through the non-adiabatic coupling vector. Clearly, the nuclear motion is necessary for transitions to take place, through the $\boldsymbol{R}(t)$ dependence of $\boldsymbol{d}_{ji}$.

The single configuration approach of Ehrenfest dynamics makes this method relatively affordable in comparison to multiconfiguration based methods. However, this evolution on mean potentials comes with drawbacks: when leaving a region of strong nonadiabatic coupling, the system does not regain its adiabaticity but is instead trapped in this mean state. This holds especially true when there is a branching of wavefunctions between different adiabatic states. This over-coherence

has been recognized and decoherence corrections have been proposed to tackle this problem (see *e.g.* references [38] and [39] for recent reviews). This makes Ehrenfest dynamics a powerful tool when investigating the relaxation from the Franck-Condon region towards regions of strong non-adiabatic coupling as discussed in chapter 3, but is less reliable when leaving this region, making full conversion into the product state impossible. For simulations of photoinduced charge separation and electron injections, as treated in chapters 4, 6 and 7, Ehrenfest dynamics are less suitable, even without taking the cost for such extended systems into account.

AO-MO quantum propagation

Simulating photoinduced processes involving extended systems become prohibitively expensive when using Ehrenfest dynamics. For the simulations of photoinduced electron injection and charge separation as discussed in chapters 4, 6 and 7, an efficient, semi-classical approach of an AO-MO quantum propagation using an Extended Hückel Hamiltonian is used that was first proposed and applied by Batista *et al.*[40] The method was first used on a static nuclear geometry, but was quickly expanded to include nuclear motion.[41–45] However, instead of using excited state nuclear dynamics, the nuclear trajectories are calculated *a priori* in the ground state. This can involve the usage of classical MD following equation 2.67, or using AIMD following equation 2.68. In this work, the trajectories are obtained via AIMD ground state dynamics using one of the semi-empirical tight binding approaches discussed earlier, DFTB or GFN-xTB. The obtained nuclear trajectories are used for the quantum electron transfer dynamics (ETD).

The time evolution of the photoexcited electronic system is done by evolving a wave packet representing the photoexcited electron and one wave packet representing the hole on these predetermined nuclear trajectories. Starting from t=0, the nuclear coordinates $\boldsymbol{R}^{t=0}$ of the first geometry determine the AOs φ and the Hamiltonian $\widehat{H}_{\mathrm{el}}^{(t=0)}$. From this, the MOs $\psi_j(\boldsymbol{r};\boldsymbol{R}^{(0)})$ with their coefficients $c_j(0)$ are obtained by solving the time independent Schrödinger equation using the Extended

Hückel approach. An appropriate wave packet Ψ is chosen to represent the photoexcited electron and hole, most often corresponding to LUMO and HOMO of the excited fragment. Using the Extended Hückel approach discussed in section 2.3, these wave packets can either be described within the diabatic atomic orbital basis as given in equations 2.48, or within the adiabatic molecular orbital basis as given in equation 2.69. For the time evolution of the wave packet, we use the adiabatic MO basis. We start from the time dependent Schrödinger equation

$$i\frac{\partial\Psi(r,t;\boldsymbol{R}(t))}{\partial t}=\widehat{H}_{\mathrm{el}}\Psi(r,t;\boldsymbol{R}(t)) \tag{2.82}$$

The electronic Hamiltonian corresponds to the Extended Hückel Hamiltonian. We insert equation 2.69 into equation 2.82 and, following the derivation as given in the beginning of section 2.5, we arrive at equation 2.71, However, since we only want to propagate on a time slice δt where the nuclear geometry is assumed to be fixed, the time dependence of $\boldsymbol{R}$ as well as the Hamiltonian is removed:

$$\begin{aligned} i\sum_{i=1}^{\infty}\frac{\partial c_i(t)\delta_{ij}}{\partial t}+i\int_{\Omega_{\mathrm{tot}}}d\boldsymbol{r}\psi_j^*(\boldsymbol{r};\boldsymbol{R}^{(\delta t)})\sum_{i=1}^{\infty}c_i(t)\frac{\partial\psi_i(\boldsymbol{r};\boldsymbol{R}^{(\delta t)})}{\partial t} \\ =\int_{\Omega_{\mathrm{tot}}}d\boldsymbol{r}\psi_j^*(\boldsymbol{r};\boldsymbol{R}^{(\delta t)})\widehat{H}_{\mathrm{el}}^{(\delta t)}\sum_{i=1}^{\infty}c_i(t)\psi_i(\boldsymbol{r};\boldsymbol{R}^{(\delta t)}) \end{aligned} \tag{2.83}$$

Since the MOs are now time independent, the second term on the left hand becomes zero and we obtain

$$i\frac{\partial c_j(t)}{\partial t}=\sum_{i=1}^{\infty}c_i(t)H_{ji}\left(\boldsymbol{R}^{(\delta t)}\right)=c_j(t)\varepsilon_i\left(\boldsymbol{R}^{(\delta t)}\right) \tag{2.84}$$

where again the off-diagonal elements of the Hamiltonian are zero due to the adiabatic, orthonormal character of the basis functions. Note that the difference to equation 2.74 and therefore to the electronic time propagation in Ehrenfest, is the dropping of the term including the non-adiabatic coupling. For a finite time slice δt, the new coefficients can then be obtained[43]:

$$c_j(\delta t) = c_j(0)e^{-i\varepsilon_j \delta t} \tag{2.85}$$

From this equation, one can see that non-adiabatic transitions are not possible within this time slice, since changes in the coefficients still lead to the same amplitude. Spatial movement of the wave packet is possible in the case of a superposition of adiabatic states, but population transfer between adiabatic states cannot occur. How are non-adiabatic transitions within this method then possible? The trick is in switching between adiabatic (MO) and diabatic (AO) representation of the wave function, as seen in scheme 2.1, where n_{BF} corresponds to the number of basis functions.

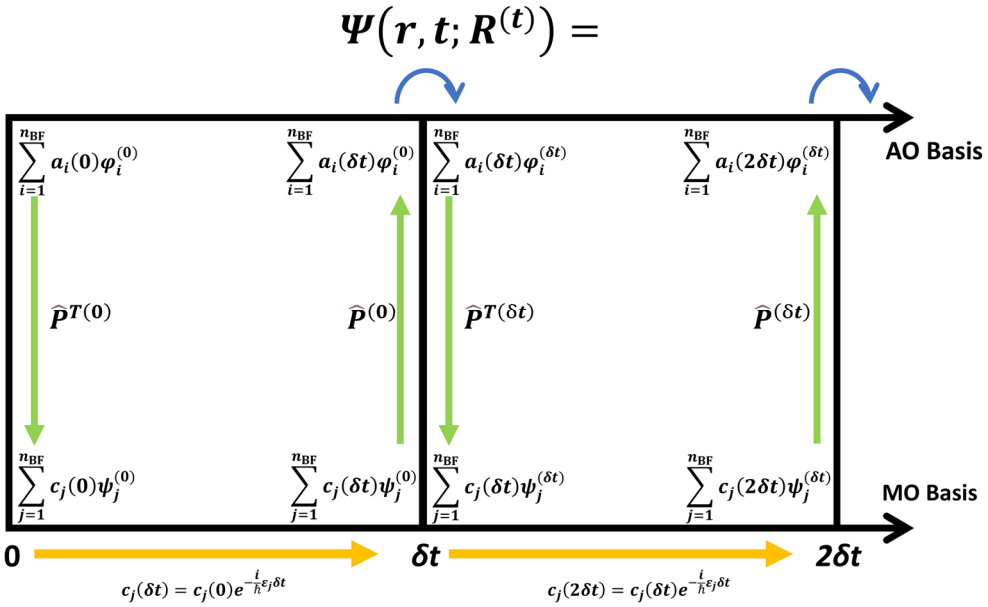

Scheme 2.1. Schematic representation of the AO/MO propagation. A wave packet representing the electron is chosen, first represented in the AO basis. After projection onto the MO basis (green arrow), the electronic time evolution is performed via the molecular orbital coefficients (orange). After projecting back onto the AO basis, the nuclei and atomic orbital basis are shifted according to the precalculated trajectory (blue). This is repeated for each consecutive time step. Note the color codes for electronic (orange) and nuclear (blue) time evolution, with green representing projection between the diabatic and adiabatic representation. Adapted from reference [43].

After the first quantum propagation of the electronic wave packet, it is projected onto the diabatic AO basis using the projection operator[43]

$$\hat{P}^{(0)}|\Psi^{(\delta t)}>=\sum_{\varphi\psi}^{n_{\mathrm{BF}}}|\varphi^{(0)}>C^{(0)}<\psi^{(0)}|, \tag{2.86}$$

where $C^{(0)}$ is the Coefficient matrix as determined by the static Extended Hückel result. The atomic orbitals are then shifted according to the new nuclear positions, assuming $|\varphi^{(0)}>\approx|\varphi^{(\delta t)}>$. The new nuclear geometry $\boldsymbol{R}^{(\delta t)}$ determines a new Hamiltonian $\hat{H}_{\mathrm{el}}^{(\delta t)}\neq\hat{H}_{\mathrm{el}}^{(0)}$, which leads to new Molecular orbitals $\psi^{(\delta t)}\neq\psi^{(0)}$.

The AO coefficients in the wave packet in the AO basis are not changed. This is where non-adiabatic transitions become possible, as the shift within the diabatic AO representation can result in changing the adiabatic state, since this wave packet in the AO representation is then projected back onto the new MO basis:

$$\hat{P}^{\mathrm{T}(\delta t)}|\Psi^{(\delta t)}>=\sum_{\varphi\psi}^{n_{\mathrm{BF}}}|\psi^{(\delta t)}>C^{\mathrm{T}(\delta t)}<\varphi^{(\delta t)}| \tag{2.87}$$

Important to note here is that the MOs as well as the coefficient matrix is different, but the AOs stay the same. This is what allows for transitions between adiabatic states. Through the change in the adiabatic MO basis, we effectively reintroduce the off-diagonal elements in the Hamiltonian matrix, since we go through the diabatic basis projecting onto a new adiabatic basis with the result of population transfer from one adiabatic state to another, which are eigenfunctions of different Hamiltonians and not orthogonal to each other.

This scheme is followed for each nuclear time step, the new nuclear positions define a new Hamiltonian and by that a new set of MOs. The wave packet is projected onto this new MO basis (see scheme 2.1). The time evolution of the MO coefficients is done following equation 2.85. After the electronic quantum propagation, the wave packet is projected back onto the AO basis and then shifted again with respect to the new coordinates. This AO-MO propagation method allows for simulating the time evolution of photoexcited electron and hole, including non-

adiabatic transitions, such as shown representatively in scheme 2.2, where a wave packet fully represented by an adiabatic state S2 evolves into S1 through non-adiabatic population transfer.

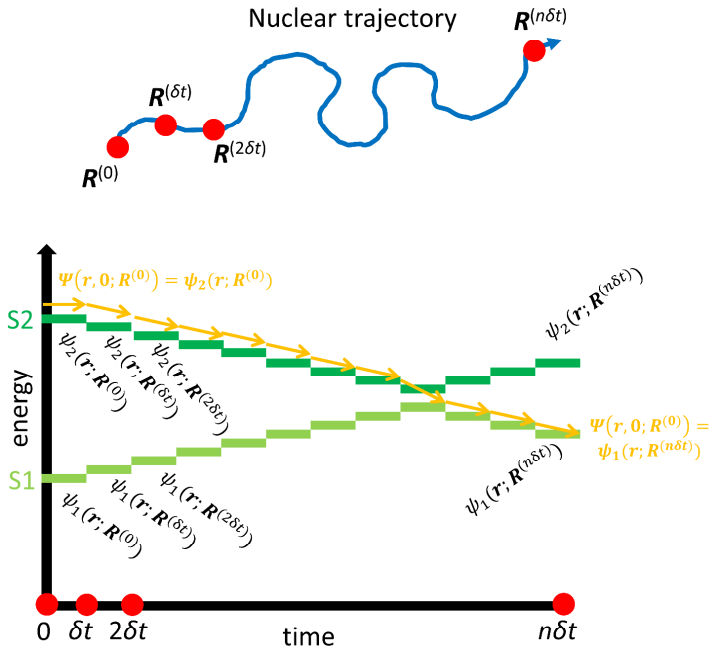

Scheme 2.2. Non-adiabatic conversion from an adiabatic state S2 to another state S1 with the AO-MO electronic propagation (yellow arrows) on a precalculated nuclear trajectory (blue arrow), starting with a wave packet equal to the adiabatic state S2. For each time step of length δt, the trajectory determines nuclear coordinates $\boldsymbol{R}^{(t)}$, which defines the molecular orbitals $\psi_i(\boldsymbol{r};\boldsymbol{R}^{(t)})$ at time t and energy of the two states S1 and S2 at the respective time step. Electronic propagation of a wave packet is performed on this MO basis. Due to the change in geometry, the wave packet is not an eigenfunction of the new Hamiltonian anymore. When the states approach each other energetically, the wave packet can only be represented by a superposition of states S2 and S1, leading to gradual population transfer between the two states. After leaving this region, the transfer is complete and the system evolves completely on state S1.

The method can be used in large, extended systems including periodic boundary conditions due to its low computational cost. It is quite reliable at elevated temperatures and large extended systems, where the approximation of the ground state trajectory is generally acceptable. Since the nuclear system evolves uninfluenced by the changed electronic structure, the electronic system cannot steer the nuclear system into resonance as with Ehrenfest dynamics. However, the electronic system can take advantage of nuclear modes available in the nuclear system due to thermal noise as shown *e.g.* in the appendix of chapter 4. All in all, the AO-MO propagator is a powerful tool for simulating photoinduced electron injection, charge transfer and charge separation in large systems in a computationally accessible way.

2.6 References

(1) Born, M.; Oppenheimer, R. Zur Quantentheorie Der Molekeln. *Ann. Phys.* **1927**, *389* (20), 457–484.

(2) Bircher, M. P.; Liberatore, E.; Browning, N. J.; Brickel, S.; Hofmann, C.; Patoz, A.; Unke, O. T.; Zimmermann, T.; Chergui, M.; Hamm, P.; Keller, U.; Meuwly, M.; Woerner, H.-J.; Vaníček, J.; Rothlisberger, U. Nonadiabatic Effects in Electronic and Nuclear Dynamics. *Struct. Dyn.* **2017**, *4* (6), 061510. https://doi.org/10.1063/1.4996816.

(3) Hohenberg, P.; Kohn, W. Inhomogeneous Electron Gas. *Phys. Rev.* **1964**, *136* (3B), B864–B871.

(4) Runge, E.; Gross, E. K. U. Density-Functional Theory for Time-Dependent Systems. *Phys. Rev. Lett.* **1984**, *52* (12), 997–1000.

(5) Car, R.; Parrinello, M. Unified Approach for Molecular Dynamics and Density-Functional Theory. *Phys. Rev. Lett.* **1985**, *55* (22), 2471–2474.

(6) Habitz, P.; Votava, C. The Hellmann–Feynman Theorem for Approximate Wave Functions and Its Application to Nonadiabatic Coupling Matrix Elements with the Aid of a Coupled Hartree–Fock Method. *J. Chem. Phys.* **1980**, *72* (10), 5532–5539. https://doi.org/10.1063/1.438971.

(7) Rabi, I. I. Space Quantization in a Gyrating Magnetic Field. *Phys. Rev.* **1937**, *51* (8), 652–654. https://doi.org/10.1103/PhysRev.51.652.

(8) Purchase, R. L.; de Groot, H. J. M. Biosolar Cells: Global Artificial Photosynthesis Needs Responsive Matrices with Quantum Coherent Kinetic Control for High Yield. *Interface focus* **2015**, *5* (3), 20150014.

(9) Akimov, A. V.; Neukirch, A. J.; Prezhdo, O. V. Theoretical Insights into Photoinduced Charge Transfer and Catalysis at Oxide Interfaces. *Chem. Rev.* **2013**, *113* (6), 4496–4565.

(10) Kohn, W.; Sham, L. J. Self-Consistent Equations Including Exchange and Correlation Effects. *Phys. Rev.* **1965**, *140* (4A), A1133–A1138.

(11) Verma, P.; Truhlar, D. G. Status and Challenges of Density Functional Theory. *Trends in Chemistry* **2020**, *2* (4), 302–318. https://doi.org/10.1016/j.trechm.2020.02.005.

(12) Becke, A. D. Density-Functional Exchange-Energy Approximation with Correct Asymptotic Behavior. *Phys. Rev. A* **1988**, *38* (6), 3098–3100.

(13) Lee, C.; Yang, W.; Parr, R. G. Development of the Colle-Salvetti Correlation-Energy Formula into a Functional of the Electron Density. *Phys. Rev. B* **1988**, *37* (2), 785–789.

(14) Perdew, J. P.; Burke, K.; Ernzerhof, M. Generalized Gradient Approximation Made Simple. *Phys. Rev. Lett.* **1996**, *77* (18), 3865–3868.

(15) Perdew, J. P.; Burke, K.; Ernzerhof, M. Generalized Gradient Approximation Made Simple [Phys. Rev. Lett. 77, 3865 (1996)]. *Phys. Rev. Lett.* **1997**, *78* (7), 1396–1396.

(16) Becke, A. D. A New Mixing of Hartree–Fock and Local Density-functional Theories. *J. Chem. Phys.* **1993**, *98* (2), 1372–1377. https://doi.org/10.1063/1.464304.

(17) Yanai, T.; Tew, D. P.; Handy, N. C. A New Hybrid Exchange–Correlation Functional Using the Coulomb-Attenuating Method (CAM-B3LYP). *Chem. Phys. Lett.* **2004**, *393* (1–3), 51–57.

(18) Akinaga, Y.; Ten-no, S. Range-Separation by the Yukawa Potential in Long-Range Corrected Density Functional Theory with Gaussian-Type Basis Functions. *Chem. Phys. Lett.* **2008**, *462* (4), 348–351. https://doi.org/10.1016/j.cplett.2008.07.103.

(19) Hückel, E. Quantentheoretische Beiträge zum Benzolproblem. I. *Z. Physik* **1931**, *70* (3), 204–286. https://doi.org/10.1007/BF01339530.

(20) Hückel, E. Quantentheoretische Beiträge zum Benzolproblem. II. *Z. Physik* **1931**, *72* (5), 310–337. https://doi.org/10.1007/BF01341953.

(21) Hückel, E. Quantentheoretische Beiträge zum Problem der aromatischen und ungesättigten Verbindungen. III. *Z. Physik* **1932**, *76* (9), 628–648. https://doi.org/10.1007/BF01341936.

(22) Hückel, E. Die freien Radikale der organischen Chemie. IV. *Z. Physik* **1933**, *83* (9), 632–668. https://doi.org/10.1007/BF01330865.

(23) Hoffmann, R. An Extended Hückel Theory. I. Hydrocarbons. *J. Chem. Phys.* **1963**, *39* (6), 1397–1412. https://doi.org/10.1063/1.1734456.
(24) Porezag, D.; Frauenheim, Th.; Köhler, Th.; Seifert, G.; Kaschner, R. Construction of Tight-Binding-like Potentials on the Basis of Density-Functional Theory: Application to Carbon. *Phys. Rev. B* **1995**, *51* (19), 12947–12957. https://doi.org/10.1103/PhysRevB.51.12947.
(25) Seifert, G.; Porezag, D.; Frauenheim, T. Calculations of Molecules, Clusters, and Solids with a Simplified LCAO-DFT-LDA Scheme. *Int. J. Quantum Chem.* **1996**, *58* (2), 185–192. https://doi.org/10.1002/(SICI)1097-461X(1996)58:2<185::AID-QUA7>3.0.CO;2-U.
(26) Elstner, M.; Porezag, D.; Jungnickel, G.; Elsner, J.; Haugk, M.; Frauenheim, Th.; Suhai, S.; Seifert, G. Self-Consistent-Charge Density-Functional Tight-Binding Method for Simulations of Complex Materials Properties. *Phys. Rev. B* **1998**, *58* (11), 7260–7268. https://doi.org/10.1103/PhysRevB.58.7260.
(27) Elstner, M.; Frauenheim, T.; Kaxiras, E.; Seifert, G.; Suhai, S. A Self-Consistent Charge Density-Functional Based Tight-Binding Scheme for Large Biomolecules. *Phys. Status Solidi B* **2000**, *217* (1), 357–376. https://doi.org/10.1002/(SICI)1521-3951(200001)217:1<357::AID-PSSB357>3.0.CO;2-J.
(28) Frauenheim, T.; Seifert, G.; Elsterner, M.; Hajnal, Z.; Jungnickel, G.; Porezag, D.; Suhai, S.; Scholz, R. A Self-Consistent Charge Density-Functional Based Tight-Binding Method for Predictive Materials Simulations in Physics, Chemistry and Biology. *Phys. Status Solidi B* **2000**, *217* (1), 41–62. https://doi.org/10.1002/(SICI)1521-3951(200001)217:1<41::AID-PSSB41>3.0.CO;2-V.
(29) Grimme, S.; Bannwarth, C.; Shushkov, P. A Robust and Accurate Tight-Binding Quantum Chemical Method for Structures, Vibrational Frequencies, and Noncovalent Interactions of Large Molecular Systems Parametrized for All Spd-Block Elements (Z = 1–86). *J. Chem. Theory Comput.* **2017**, *13* (5), 1989–2009. https://doi.org/10.1021/acs.jctc.7b00118.
(30) Grimme, S.; Antony, J.; Ehrlich, S.; Krieg, H. A Consistent and Accurate Ab Initio Parametrization of Density Functional Dispersion Correction (DFT-D) for the 94 Elements H-Pu. *J. Chem. Phys.* **2010**, *132* (15), 154104. https://doi.org/10.1063/1.3382344.
(31) Grimme, S.; Ehrlich, S.; Goerigk, L. Effect of the Damping Function in Dispersion Corrected Density Functional Theory. *J. Comput. Chem.* **2011**, *32* (7), 1456–1465. https://doi.org/10.1002/jcc.21759.
(32) van Duin, A. C. T.; Dasgupta, S.; Lorant, F.; Goddard, W. A. ReaxFF: A Reactive Force Field for Hydrocarbons. *J. Phys. Chem. A* **2001**, *105* (41), 9396–9409. https://doi.org/10.1021/jp004368u.
(33) Tully, J. C. Nonadiabatic Dynamics. In *Modern Methods for Multidimensional Dynamics Computations in Chemistry*; World Scientific, 1998. https://doi.org/10.1142/3672.
(34) Tully, J. C. Mixed Quantum–Classical Dynamics. *Faraday Discuss.* **1998**, *110* (0), 407–419. https://doi.org/10.1039/A801824C.
(35) Curchod, B. F. E.; Rothlisberger, U.; Tavernelli, I. Trajectory-Based Nonadiabatic Dynamics with Time-Dependent Density Functional Theory. *Chem. Phys. Chem.* **2013**, *14* (7), 1314–1340.
(36) Beck, M. The Multiconfiguration Time-Dependent Hartree (MCTDH) Method: A Highly Efficient Algorithm for Propagating Wavepackets. *Physics Reports* **2000**, *324* (1), 1–105. https://doi.org/10.1016/S0370-1573(99)00047-2.
(37) Worth, G. A.; Meyer, H.-D.; Köppel, H.; Cederbaum, L. S.; Burghardt, I. Using the MCTDH Wavepacket Propagation Method to Describe Multimode Non-Adiabatic Dynamics. *International Reviews in Physical Chemistry* **2008**, *27* (3), 569–606. https://doi.org/10.1080/01442350802137656.
(38) Crespo-Otero, R.; Barbatti, M. Recent Advances and Perspectives on Nonadiabatic Mixed Quantum–Classical Dynamics. *Chem. Rev.* **2018**, *118* (15), 7026–7068. https://doi.org/10.1021/acs.chemrev.7b00577.
(39) Nelson, T. R.; White, A. J.; Bjorgaard, J. A.; Sifain, A. E.; Zhang, Y.; Nebgen, B.; Fernandez-Alberti, S.; Mozyrsky, D.; Roitberg, A. E.; Tretiak, S. Non-Adiabatic Excited-State Molecular Dynamics: Theory and Applications for Modeling Photophysics in Extended Molecular

Materials. *Chem. Rev.* **2020**, *120* (4), 2215–2287. https://doi.org/10.1021/acs.chemrev.9b00447.

(40) Rego, L. G. C.; Batista, V. S. Quantum Dynamics Simulations of Interfacial Electron Transfer in Sensitized TiO $_2$ Semiconductors. *J. Am. Chem. Soc.* **2003**, *125* (26), 7989–7997. https://doi.org/10.1021/ja0346330.

(41) Hoff, D. A.; Silva, R.; Rego, L. G. C. Subpicosecond Dynamics of Metal-to-Ligand Charge-Transfer Excited States in Solvated [Ru(Bpy)3]2+ Complexes. *J. Phys. Chem. C* **2011**, *115* (31), 15617–15626. https://doi.org/10.1021/jp2022715.

(42) Hoff, D. A.; da Silva, R.; Rego, L. G. C. Coupled Electron–Hole Quantum Dynamics on D–π–A Dye-Sensitized TiO $_2$ Semiconductors. *J. Phys. Chem. C* **2012**, *116* (40), 21169–21178. https://doi.org/10.1021/jp303647x.

(43) da Silva, R.; Hoff, D. A.; Rego, L. G. C. Coupled Quantum-Classical Method for Long Range Charge Transfer: Relevance of the Nuclear Motion to the Quantum Electron Dynamics. *J. Phys.: Condens. Matter* **2015**, *27* (13), 134206. https://doi.org/10.1088/0953-8984/27/13/134206.

(44) Monti, A.; Negre, C. F. A.; Batista, V. S.; Rego, L. G. C.; de Groot, H. J. M.; Buda, F. Crucial Role of Nuclear Dynamics for Electron Injection in a Dye–Semiconductor Complex. *J. Phys. Chem. Lett.* **2015**, *6* (12), 2393–2398.

(45) da Silva Oliboni, R.; Bortolini, G.; Torres, A.; Rego, L. G. C. A Nonadiabatic Excited State Molecular Mechanics/Extended Hückel Ehrenfest Method. *J. Phys. Chem. C* **2016**, *120* (48), 27688–27698. https://doi.org/10.1021/acs.jpcc.6b09606.